Molecular Cell

Article

Mrc1 regulates parental histone segregation and heterochromatin inheritance

Graphical abstract

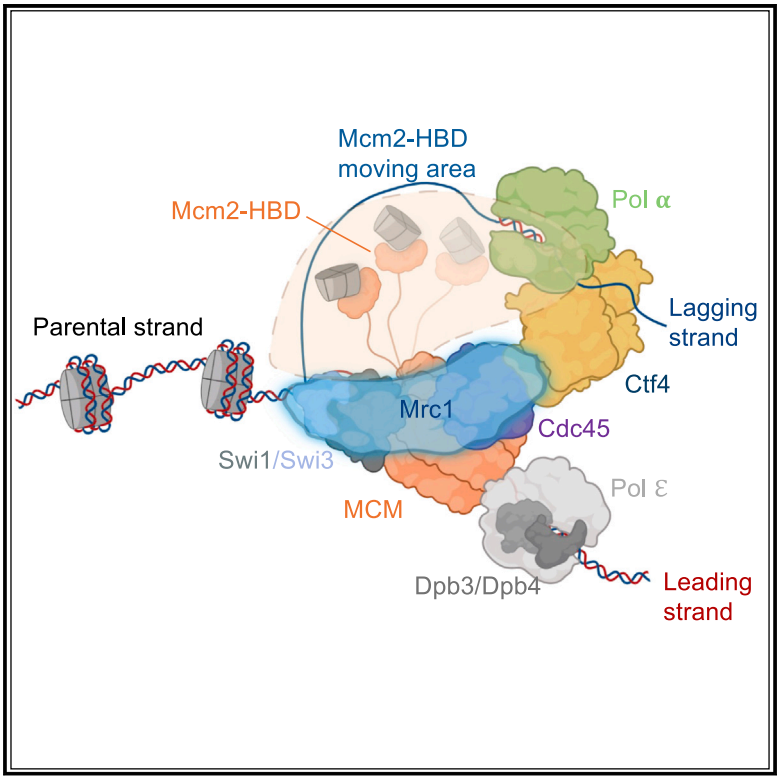

Authors

Takenori Toda, Yimeng Fang, Chun-Min Shan, ..., Feng Qiao, Zhiguo Zhang, Songtao Jia

Correspondence

shancm@im.ac.cn (C.-M.S.), songtao.jia@columbia.edu (S.J.)

In brief

The symmetrical segregation of parental histones to daughter strands during DNA replication is critical for chromatin-based epigenetic inheritance. Toda et al. discover that replisome protein Mrc1, which is required for DNA replication checkpoint activation and replisome speed progression, is also essential for symmetrical parental histone segregation and proper heterochromatin inheritance.

Highlights

- Mrc1 is required for epigenetic inheritance of heterochromatin
- Mrc1 is required for parental histone transfer to the lagging strand
- Mrc1 facilitates parental histone transfer between Mcm2 and Pol alpha
- Mrc1-Mcm2 interaction is critical for parental histone transfer

Toda et al., 2024, Molecular Cell *84*, 1–14
September 5, 2024
https://doi.org/10.1016/j.molcel.2024.07.002

CellPress

Please cite this article in press as: Toda et al., Mrc1 regulates parental histone segregation and heterochromatin inheritance, Molecular Cell (2024), https://doi.org/10.1016/j.molcel.2024.07.002

Molecular Cell

CellPress

Article

Mrc1 regulates parental histone segregation and heterochromatin inheritance

Takenori Toda,[1,5] Yimeng Fang,[1,5] Chun-Min Shan,[1,2,5,*] Xu Hua,[3] Jin-Kwang Kim,[4] Lauren Clarissa Tang,[1] Marko Jovanovic,[1] Liang Tong,[1] Feng Qiao,[4] Zhiguo Zhang,[3] and Songtao Jia[1,6,*]

[1]Department of Biological Sciences, Columbia University, New York, NY 10027, USA
[2]State Key Laboratory of Plant Genomics, Institute of Microbiology, Chinese Academy of Sciences, Beijing 100101, China
[3]Institute for Cancer Genetics, Department of Pediatrics, and Department of Genetics and Development, Columbia University Irving Medical Center, New York, NY 10032, USA
[4]Department of Biological Chemistry, School of Medicine, University of California, Irvine, CA 92697, USA
[5]These authors contributed equally
[6]Lead contact
*Correspondence: shancm@im.ac.cn (C.-M.S.), songtao.jia@columbia.edu (S.J.)
https://doi.org/10.1016/j.molcel.2024.07.002

SUMMARY

Chromatin-based epigenetic memory relies on the symmetric distribution of parental histones to newly synthesized daughter DNA strands, aided by histone chaperones within the DNA replication machinery. However, the mechanism of parental histone transfer remains elusive. Here, we reveal that in fission yeast, the replisome protein Mrc1 plays a crucial role in promoting the transfer of parental histone H3-H4 to the lagging strand, ensuring proper heterochromatin inheritance. In addition, Mrc1 facilitates the interaction between Mcm2 and DNA polymerase alpha, two histone-binding proteins critical for parental histone transfer. Furthermore, Mrc1's involvement in parental histone transfer and epigenetic inheritance is independent of its known functions in DNA replication checkpoint activation and replisome speed control. Instead, Mrc1 interacts with Mcm2 outside of its histone-binding region, creating a physical barrier to separate parental histone transfer pathways. These findings unveil Mrc1 as a key player within the replisome, coordinating parental histone segregation to regulate epigenetic inheritance.

INTRODUCTION

Eukaryotic cells fold their genomic DNA with histone proteins into chromatin. The nucleosome is the fundamental unit of chromatin and consists of 147 base pairs of DNA wrapped around an octamer of histones, including two each of H2A, H2B, H3, and H4. Covalent modifications of histones are crucial for regulating chromatin structure and establishing gene expression programs. Some of these modifications, such as the tri-methylation of histone H3 lysine 9 (H3K9me3) or trimethylation of histone H3 lysine 27 (H3K27me3), can be passed down to the subsequent generation of cells, forming an epigenetic memory.[1,2]

DNA replication coupled nucleosome assembly plays a crucial role in the inheritance of epigenetic information.[1,2] During this process, the advancing replication fork disrupts parental nucleosomes. Parental H3-H4 tetramers, with their modifications, are deposited at their original locations[3–5] and distributed symmetrically between the two daughter strands to guide nucleosome formation.[6–8] Additionally, newly synthesized H3-H4, which lacks parental modifications, are also incorporated into replicated DNA to fill the gaps. The modifications on parental H3-H4 can serve as the epigenetic template, as certain histone-modifying enzymes can recognize the modifications they create. For example, fission yeast H3K9 methyltransferase Clr4 contains both a catalytic SET (Su(var)3-9, ehancer of zeste, and Trithorax)domain responsible for methylating H3K9 as well as a chromodomain that recognizes H3K9me3.[9–11] Parental histones containing H3K9me3 recruit Clr4 to modify adjacent newly synthesized H3, thus replenishing H3K9me3 to original levels on both daughter strands.[9,12]

The distribution of parental H3-H4 tetramers to daughter strands is orchestrated by various histone-binding proteins within the DNA replication machinery.[1] Specifically, the Dpb3/Dpb4 (POLE3/POLE4) subunits of DNA polymerase epsilon facilitate the deposition of parental histone H3-H4 to the leading strand.[6] On the other hand, the Mcm2 subunit of the replicative helicase and the largest subunit of DNA polymerase alpha, both possessing histone-binding domains (HBDs), are responsible for depositing parental histone H3-H4 to the lagging strand.[7,8,13] The roles of Dpb3/Dpb4 and Pol alpha in parental histone H3-H4 transfer are in alignment with their positions on the leading and lagging strand, respectively.[14–17] However, the mechanism by which the leading strand anchored Mcm2 promotes parental histone H3-H4 transfer to the lagging strand remains elusive. Unfortunately, investigating

Please cite this article in press as: Toda et al., Mrc1 regulates parental histone segregation and heterochromatin inheritance, Molecular Cell (2024), https://doi.org/10.1016/j.molcel.2024.07.002

the mechanism of parental histone transfer is hindered by the lack of genetic screens to discover additional regulators specifically associated with this process.

Heterochromatin formation in the fission yeast, *Schizosaccharomyces pombe*, has been a valuable model for studying epigenetic inheritance.[18–21] In this organism, large heterochromatin domains enriched with H3K9me3 are found at pericentric regions, sub-telomeres, and the silent mating-type region. The process of heterochromatin formation consists of two distinct steps: initiation and inheritance (also referred to as maintenance). During initiation, Clr4 is recruited to these regions either through the RNA interference (RNAi) machinery or DNA binding proteins, leading to *de novo* heterochromatin formation. In the inheritance step, parental histone H3-H4 deposited on daughter strands serve as a platform for recruiting Clr4, thereby replenishing H3K9me3 levels in a self-templated process. The genetic separation of these two steps has yielded reporter genes that have been pivotal in elucidating the mechanism of chromatin-based epigenetic inheritance. For example, at the silent mating-type region, removal of the *cenH* sequence (*KΔ*) disrupts RNAi-mediated heterochromatin initiation while still allowing faithful inheritance of the mating-type region heterochromatin.[22,23] In addition, an ectopic heterochromatin created by targeting a Clr4-SET domain-TetR fusion protein (TetR-Clr4-I) to *tetO* binding sites can be stably inherited in certain genetic contexts after TetR-Clr4-I is removed from its target sites.[24,25] Using these inheritance-specific reporter assays, we have demonstrated that a mutation in the Mcm2-HBD leads to strong defects of heterochromatin inheritance,[26] suggesting that the proper segregation of parental histone H3-H4 is indeed critical for heterochromatin inheritance.

Here, using an inheritance-specific assay, we screened the fission yeast deletion library for additional regulators of heterochromatin inheritance. We identified Mrc1, a replisome component known for controlling replication fork speed and activating the DNA replication checkpoint under replication stress, as a critical factor for epigenetic inheritance. Furthermore, we demonstrate that the interaction between Mrc1 and Mcm2 directs the Mcm2-HBD to the proximity of Pol alpha, thereby facilitating the deposition of parental histone H3-H4 to the lagging strand during DNA replication.

RESULTS

Mrc1 is required for heterochromatin inheritance

To gain insight into the mechanisms governing epigenetic inheritance, we screened the fission yeast deletion library for mutations that disrupt silencing of *KΔ::ade6*$^+$, a reporter created by replacing the *cenH* sequence at the silent mating-type region with an *ade6*$^+$ gene (Figure 1A). When *KΔ::ade6*$^+$ is silenced, cells form red colonies on a low adenine medium (YE, yeast extract), indicating proper heterochromatin inheritance. Conversely, when heterochromatin inheritance is impaired, *KΔ::ade6*$^+$ is expressed, and cells form white colonies on YE medium. The clear difference in colony color due to reporter gene expression provides a highly sensitive assay for the identification of mutations that impact epigenetic inheritance.

Our screen successfully identified mutations in various components of the Clr4 complex, HP1 proteins, and histone deacetylases, all of which have well-established roles in heterochromatin inheritance (Figures 1B and 1C). Notably, we discovered Mrc1, a highly conserved protein that plays diverse roles in DNA replication and DNA replication checkpoint activation, is required for the silencing of *KΔ::ade6*$^+$. The mammalian homolog of Mrc1, Claspin, is misregulated in various types of cancer,[27] underscoring the importance of this protein family in regulating cellular functions. It is interesting to note that *mrc1* mutations were also identified in an independent screen for factors that affect heterochromatin inheritance.[28]

To validate the findings of our screen, we constructed an *mrc1Δ KΔ::ade6*$^+$ strain through a genetic cross. Serial dilution analyses confirm that *mrc1Δ* indeed results in defective silencing of *KΔ::ade6*$^+$, evident from the formation of white/pink colonies on YE medium (Figure 1D, left). Furthermore, chromatin immunoprecipitation-quantitative PCR (ChIP-qPCR) analyses demonstrate that H3K9me3 levels at *KΔ::ade6*$^+$ are strongly reduced in *mrc1Δ* cells, similar to those in *clr4Δ* cells (Figure 1D, right).

We also investigated the role of Mrc1 in epigenetic inheritance by examining the inheritance of an ectopic heterochromatin. Targeting of TetR-Clr4-I to *tetO* binding sites results in the formation of an ectopic H3K9me3 domain and the silencing of an adjacent *gfp*$^+$ reporter gene.[24] Removal of TetR-Clr4-I from *tetO* by using tetracycline prevents initiation but allows the inheritance of the silenced state through endogenous Clr4 and parental histones, when the histone demethylase Epe1 is absent (Figure 1E). In *epe1Δ* cells, low levels of GFP expression are sustained even after 24 h of tetracycline addition (Figure 1F). ChIP analyses further demonstrate a gradual and mild decay of H3K9me3 levels at the *tetO* locus (Figure 1G). By contrast, *epe1Δ mrc1Δ* cells exhibit a more rapid activation of GFP expression and a swifter loss of H3K9me3 at *tetO* during the same time frame (Figures 1F and 1G).

To investigate whether Mrc1 is specifically involved in epigenetic inheritance, we also tested its effects on endogenous heterochromatin at the pericentric region. Here, the *dg* and *dh* repeat sequences initiate heterochromatin formation via the RNAi pathway.[29] An *ade6*$^+$ reporter inserted at pericentric repeats (*otr::ade6*$^+$) is effectively silenced in wild-type cells, resulting in red colonies on YE medium (Figures 1H and 1I). By contrast, *clr4Δ* cells exhibit strong silencing defects, generating white colonies, while *mrc1Δ* cells only display mild silencing defects, leading to dark pink colonies (Figure 1I, left). Furthermore, ChIP analyses reveal only a slight reduction in H3K9me3 levels at *dh* in *mrc1Δ* cells as compared with a complete loss of H3K9me3 in *clr4Δ* cells (Figure 1I, right). The ribonuclease Dicer (Dcr1) is critical for processing repeat transcripts and generating small interfering RNAs, which initiate heterochromatin formation at pericentric repeats (Figure S1A).[29,30] ChIP analyses show that H3K9me3 levels at pericentric *dh* repeats decrease in *dcr1Δ* cells and further decrease in *mrc1Δ dcr1Δ* cells (Figure S1B). These results indicate that Mrc1 collaborates with the RNAi pathway to regulate heterochromatin assembly at endogenous pericentric regions.

Overall, these results suggest that Mrc1 plays a specific role in heterochromatin inheritance. However, at endogenous heterochromatin regions, other pathways involved in heterochromatin initiation mask defects associated with the loss of Mrc1-mediated heterochromatin inheritance.

Please cite this article in press as: Toda et al., Mrc1 regulates parental histone segregation and heterochromatin inheritance, Molecular Cell (2024), https://doi.org/10.1016/j.molcel.2024.07.002

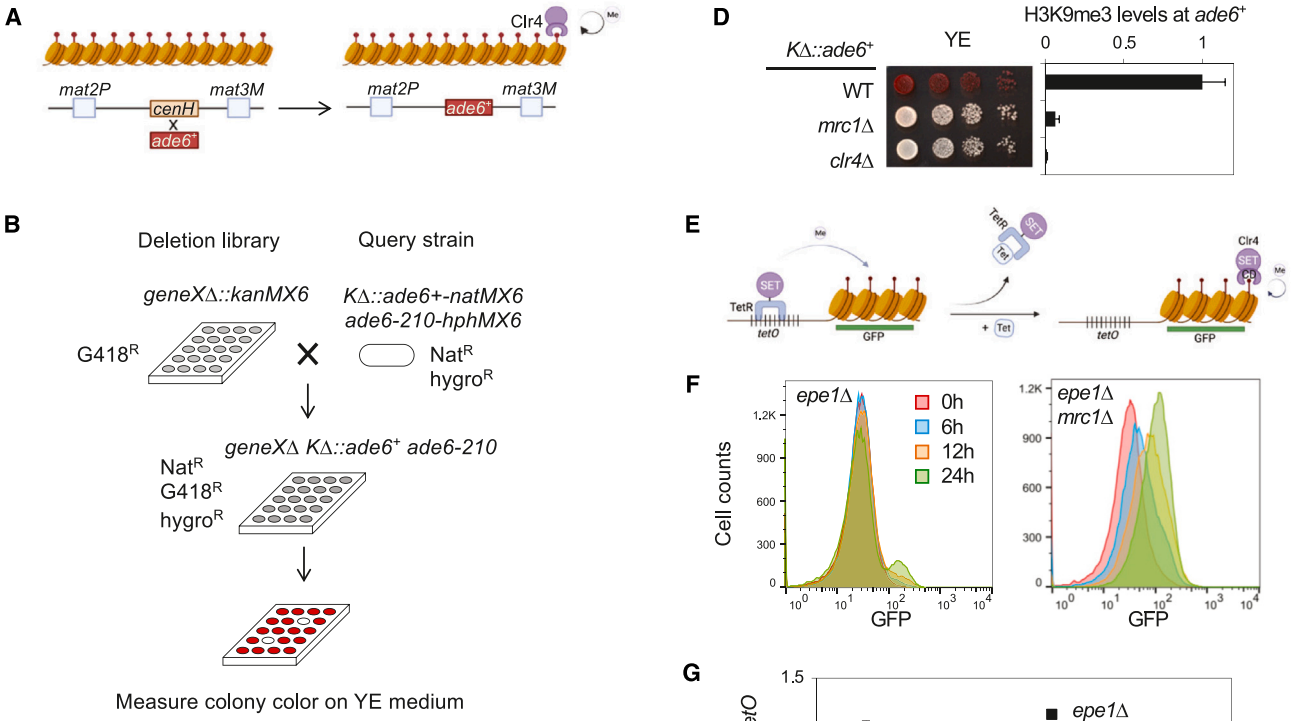

C

Gene	Description
clr4	H3K9 methyltransferase CLRC
rik1	H3K9 methyltransferase CLRC
raf1	H3K9 methyltransferase CLRC
raf2	H3K9 methyltransferase CLRC
swi6	HP1
sir2	HDAC
clr1	HDAC (SHREC)
clr2	HDAC (SHREC)
clr3	HDAC (SHREC)
alp13	HDAC (Clr6 complex)
clr5	silencing protein
meu6	gene next to *clr4*
ade3	adenine synthesis
ade4	adenine synthesis
ade5	adenine synthesis
pof3	protein ubiquitination
mrc1	DNA replication machinery

Figure 1. Mrc1 is critical for epigenetic inheritance of heterochromatin

(A) Schematic diagram of the *KΔ::ade6*$^+$ reporter.

(B) Schematic diagram of a high-throughput screen with the fission yeast deletion library for mutations that affect silencing of *KΔ::ade6*$^+$.

(C) List of mutations identified from the screen.

(D) Left, serial dilution analysis of indicated strains to measure the expression of *KΔ::ade6*$^+$. Right, chromatin immunoprecipitation (ChIP) analysis of H3K9me3 level at the *KΔ::ade6*$^+$, normalized to *act1*$^+$. Data are presented as mean ± SD of three technical replicates.

(E) Schematic diagram of the *tetO::gfp*$^+$ reporter.

(F) Flow cytometry analysis of GFP expression at different time points after tetracycline addition.

(G) ChIP analysis of H3K9me3 level at *tetO*, normalized to *act1*$^+$. Data are presented as mean ± SD of three technical replicates.

(H) Schematic diagram of the *otr::ade6*$^+$ reporter.

(I) Left, serial dilution analysis of indicated strains to measure the expression of *otr::ade6*$^+$. Right, ChIP analysis of H3K9me3 level at pericentric *dh* repeats, normalized to *act1*$^+$. Data are presented as mean ± SD of three technical replicates. Number on the right indicates two-tailed *p* value of unpaired t test.

See also Figure S1.

Please cite this article in press as: Toda et al., Mrc1 regulates parental histone segregation and heterochromatin inheritance, Molecular Cell (2024), https://doi.org/10.1016/j.molcel.2024.07.002

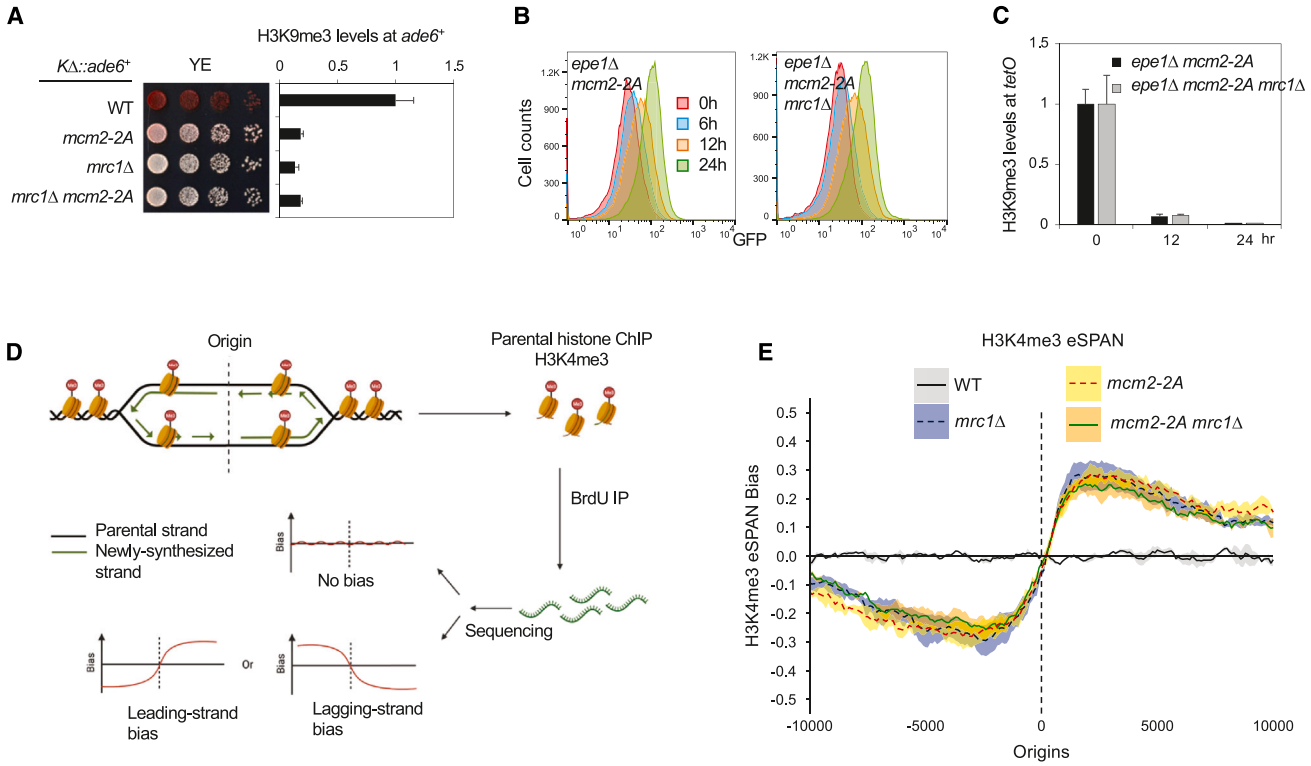

Figure 2. Mrc1 functions together with Mcm2 to regulate parental histone segregation

(A) Left, serial dilution analysis of indicated strains to measure the expression of *KΔ::ade6*$^+$. Right, ChIP analysis of H3K9me3 level at the *KΔ::ade6*$^+$, normalized to *act1*$^+$. Data are presented as mean ± SD of three technical replicates.

(B) Flow cytometry analysis of GFP expression at different time points after tetracycline addition.

(C) ChIP analysis of H3K9me3 level at *tetO*, normalized to *act1*$^+$. Data are presented as mean ± SD of three technical replicates.

(D) Schematic diagram of the eSPAN procedure and possible outcomes.

(E) eSPAN analysis of H3K4me3 bias levels at replication origins. The shading of the bias line plot is the 95% confidence interval of the mean value of at least two biological replicates, which is about mean ± 2 folds of the standard error.

Mrc1 is required for the deposition of parental histones to the lagging strand

We have demonstrated that in fission yeast, mutating two residues within the Mcm2 HBD that are critical for interaction with histone H3-H4 (Y81A and Y89A, referred to as *mcm2-2A* hereafter)[31,32] hinders the segregation of parental histones to the lagging strand and results in defective heterochromatin inheritance.[26] We found that *mrc1Δ* and *mcm2-2A mrc1Δ* cells behave similarly to *mcm2-2A* cells in the silencing of *KΔ::ade6*$^+$ (Figure 2A). In addition, *epe1Δ mrc1Δ* and *epe1Δ mcm2-2A mrc1Δ* cells behave similarly to *epe1Δ mcm2-2A* cells in the inheritance of *tetO-gfp*$^+$ (Figures 2B and 2C). These results suggest that Mrc1 and Mcm2-HBD function in the same pathway.

Considering that Mrc1 is a component of the DNA replication machinery and that *mrc1Δ* phenocopies *mcm2-2A*, we further investigated whether Mrc1 is required for parental histone H3-H4 segregation by using enrichment and sequencing of protein-associated nascent DNA (eSPAN), a technique that allows us to discern the distribution of proteins to the leading and lagging strands at the replication fork.[6,7,17,26] We synchronized fission yeast cells at the G2/M phase using a *cdc25-22* temperature-sensitive mutant and added bromodeoxyuridine (BrdU) before the S phase to label newly synthesized DNA.[33,34] We then performed ChIP using an antibody against H3K4me3, a marker for parental histones enriched at replication origins,[6,7] followed by a second round of immunoprecipitation with an antibody against BrdU to enrich newly replicated single-strand DNA (ssDNA) associated with H3K4me3 for next-generation sequencing. The eSPAN signals at replication origins allow the detection of parental histone H3-H4 deposition on the two daughter strands during DNA replication (Figure 2D).[6,7,26] We found that wild-type cells show a relatively balanced distribution of parental histone H3-H4 toward the two strands at replication origins (Figure 2E), consistent with studies in budding yeast and mouse embryonic stem cells.[6–8,13] Interestingly, *mrc1Δ* cells display a strong leading-strand H3K4me3 eSPAN bias, similar to *mcm2-2A* cells (Figure 2E), suggesting that Mrc1 and Mcm2 facilitate the deposition of parental histone H3-H4 to the lagging strand. Moreover, *mcm2-2A mrc1Δ* cells show similar levels of H3K4me3 eSPAN bias as *mrc1Δ* or *mcm2-2A* cells (Figure 2E), consistent with the idea that they function in the same pathway.

Please cite this article in press as: Toda et al., Mrc1 regulates parental histone segregation and heterochromatin inheritance, Molecular Cell (2024), https://doi.org/10.1016/j.molcel.2024.07.002

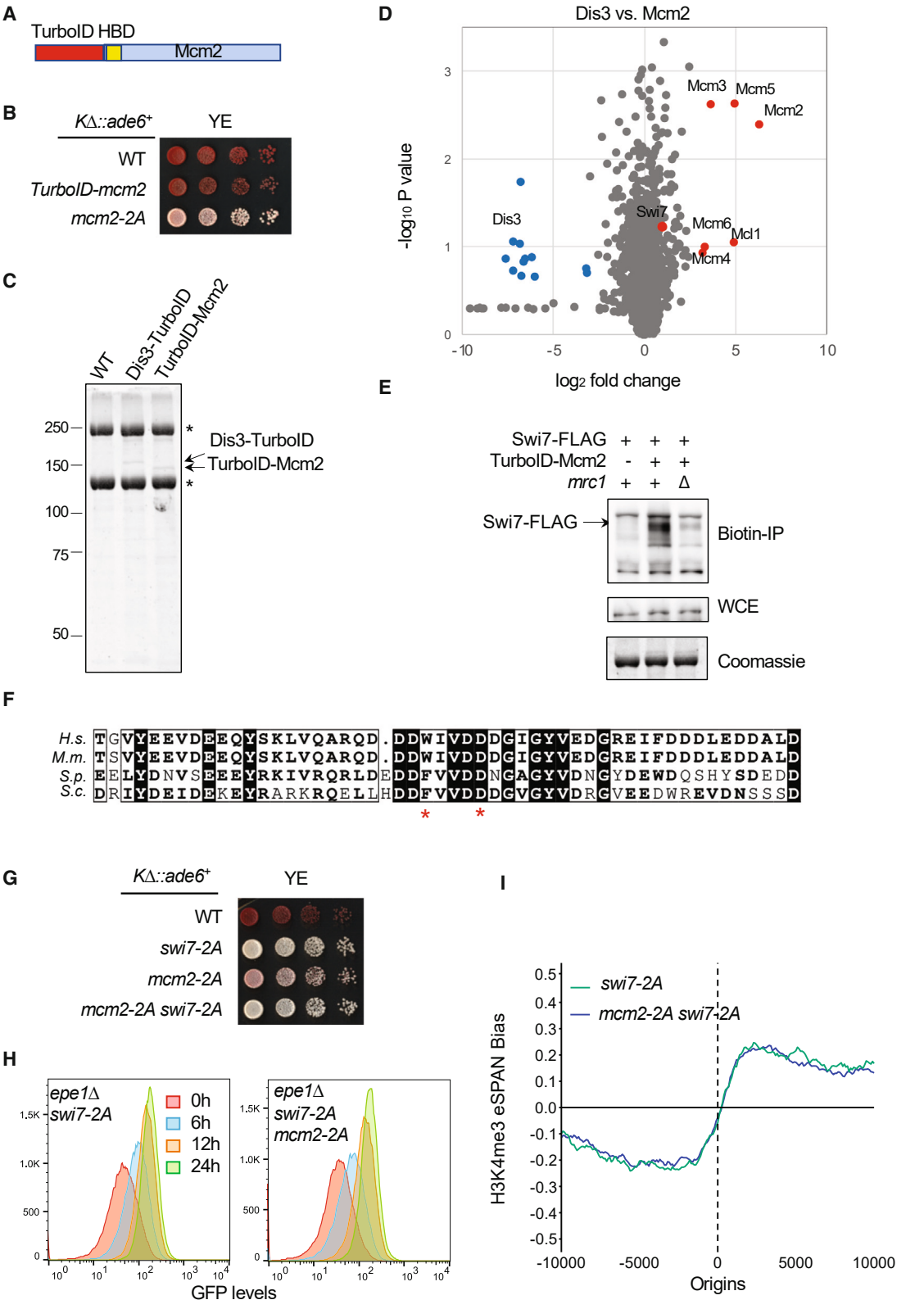

(legend on next page)

Please cite this article in press as: Toda et al., Mrc1 regulates parental histone segregation and heterochromatin inheritance, Molecular Cell (2024), https://doi.org/10.1016/j.molcel.2024.07.002

Mrc1 is required for the biotinylation of DNA polymerase alpha by TurboID-Mcm2

To gain insights into the mechanism by which Mrc1 regulates Mcm2-mediated parental histone H3-H4 segregation to the lagging strand, we employed proximity-dependent protein biotinylation[35] to examine Mcm2-HBD protein interactions. We introduced TurboID at the N terminus of Mcm2, adjacent to the HBD, at the endogenous *mcm2*$^+$ locus (Figure 3A). The insertion of TurboID has no effects on the silencing of *KΔ::ade6*$^+$, indicating that it does not interfere with the function of Mcm2 in heterochromatin inheritance (Figure 3B). We then used Strep-Tactin to isolate biotinylated proteins, with a parallel purification of Dis3-TurboID serving as a control for non-specific protein biotinylation in the nucleus.[36] Coomassie blue staining of Strep-Tactin purified fractions reveals bands specific to Dis3 and Mcm2, consistent with strong self-biotinylation (Figure 3C). Mass spectrometry analysis of Dis3-TurboID demonstrates enrichment of exosome components, including Csl4, Dis3, Mtr3, Red1, Rrp6, RRp40, Rrp42, Rrp45, and Ski6, consistent with a previous study[35] (Figure 3D; Table S1). By contrast, TurboID-Mcm2 shows enrichment of Mcm2, Mcm3, Mcm4, Mcm5, Mcm6, and Mcl1 (homolog of budding yeast Ctf4) (Figure 3D; Table S1). Notably, the levels of each protein enriched are generally in agreement with their proximity to Mcm2-HBD based on structural studies,[14,16,37] consistent with the idea that Mcm2-HBD is on a path to transfer parental histones to the rear of the replisome on the lagging strand. They also demonstrate the ability of TurboID-mediated biotinylation to discern protein interaction changes within the replisome.

We also detected biotinylated Swi7 (fission yeast DNA polymerase alpha largest subunit) in TurboID-Mcm2 mass spectrometry analysis, suggesting that Mcm2 can reach the vicinity of Swi7 (Figure 3D; Table S1). Western blot analyses of strep-Tactin purified fractions confirm specific biotinylation of Swi7 by TurboID-Mcm2, with reduced biotinylation levels in *mrc1Δ* cells (Figure 3E), suggesting that Mrc1 brings Mcm2 and Swi7 into proximity.

The proper transfer of parental histones to the lagging strand also requires the HBD of DNA polymerase alpha in budding yeast and mammals[7,13] and Mcm2-HBD interacts with Swi7-HBD in budding yeast.[38] To confirm the role of the Swi7-HBD in epigenetic inheritance and parental histone H3-H4 transfer in fission yeast, we introduced mutations in conserved residues within the Swi7-HBD for histone interaction (F61A and D65A, referred to as *swi7-2A* hereafter) (Figure 3F) into the endogenous *swi7*$^+$ locus. We observed compromised silencing of *KΔ::ade6*$^+$ in *swi7-2A* and *mcm2-2A swi7-2A* cells, similar to *mcm2-2A* cells (Figure 3G). In addition, *epe1Δ swi7-2A* and *epe1Δ mcm2-2A swi7-2A* cells behave similarly to *epe1Δ mcm2-2A* cells in the inheritance of *tetO-gfp*$^+$ (Figure 3H). Moreover, *mcm2-2A*, *swi7-2A*, and *mcm2-2A swi7-2A* cells show similar levels of H3K4me3 eSPAN bias (Figure 3I). Therefore, Mcm2-HBD, Swi7-HBD, and Mrc1 function in the same lagging strand parental histone H3-H4 deposition pathway, and Mrc1 might facilitate the transfer of parental histone H3-H4 from Mcm2-HBD to Swi7-HBD.

The role of Mrc1 in heterochromatin inheritance is independent of its DNA replication checkpoint function

Fission yeast Mrc1 plays a crucial role in activating the DNA replication checkpoint by facilitating the phosphorylation of Cds1 (Rad53 in budding yeast and Chk1 in mammals) by Rad3 (Mec1 in budding yeast and ATR (ataxia-telangiectasia-mutated and Rad3-related) in mammals) under replication stress (Figure 4A).[39,40] Mrc1 itself is phosphorylated by Rad3, and this phosphorylation is critical for the activation of Cds1.[41] Mutants such as *rad3Δ*, *cds1Δ*, or *mrc1-6A*, which contains mutations of Rad3 phosphorylation sites,[41] are defective in replication checkpoint activation and are highly sensitive to hydroxyurea (HU), a ribonucleotide reductase inhibitor (Figure 4B).[39,41] However, these mutations do not affect the silencing of *KΔ::ade6*$^+$ or the inheritance of silenced *tetO-gfp*$^+$ after TetR-Clr4-I removal (Figures 4B and 4C), suggesting that Mrc1's role in heterochromatin inheritance is independent of its function in the replication checkpoint.

Mrc1 is also part of the replication fork protection complex (FPC), which facilitates fork restart in the presence of DNA damage and speeds up DNA replication.[16,42,43] The FPC includes two additional components, Swi1 and Swi3 (Tof1 and Csm3 in budding yeast and Timeless and Tipin in mammals) (Figure 4A).[44] Although *swi1Δ* or *swi3Δ* mildly affect the silencing of *KΔ::ade6*$^+$ and the inheritance of *tetO-gfp*$^+$ after TetR-Clr4-I removal (Figures 4B and 4C), their effects are much weaker compared with *mrc1Δ*. These results suggest that the function of Mrc1 in heterochromatin inheritance is largely independent of FPC.

Mapping regions of Mrc1 required for heterochromatin inheritance

Mrc1 does not possess clearly defined domains, and cryoelectron microscopy (cryo-EM) studies of budding yeast and human replisome have been unable to determine the structure of Mrc1/Claspin, suggesting that it is highly flexible.[14,16] To investigate how Mrc1 regulates heterochromatin inheritance, we mapped the region of Mrc1 responsible for this function by generating a series of large truncations at the endogenous *mrc1*$^+$ locus

Figure 3. Mrc1 regulates the proximity between Mcm2-HBD and Swi7

(A) Diagram of TurboID-Mcm2.
(B) Serial dilution analysis of indicated strains to measure the expression of *KΔ::ade6*$^+$.
(C) SDS-PAGE and Coomassie blue staining of Strep-Tactin purified fractions. The positions of Dis3-TurboID and TurboID-Mcm2 are indicated. * represents prominent endogenously biotinylated proteins.
(D) Volcano plot of Dis3-TurboID and TurboID-Mcm2 purifications.
(E) Top, western blot analysis of Strep-Tactin purified fractions with a FLAG antibody. Middle, western blot analysis of whole-cell extract (WCE) with a FLAG antibody. Bottom, Coomassie blue stain of Strep-Tactin purified fractions.
(F) Sequence alignment of the histone-binding domain of the largest subunit of Pol alpha. Red stars indicate residues critical for histone binding.
(G) Serial dilution analysis of indicated strains to measure the expression of *KΔ::ade6*$^+$.
(H) Flow cytometry analysis of GFP expression at different time points after tetracycline addition.
(I) eSPAN analysis of H3K4me3 bias levels at replication origins.

Please cite this article in press as: Toda et al., Mrc1 regulates parental histone segregation and heterochromatin inheritance, Molecular Cell (2024), https://doi.org/10.1016/j.molcel.2024.07.002

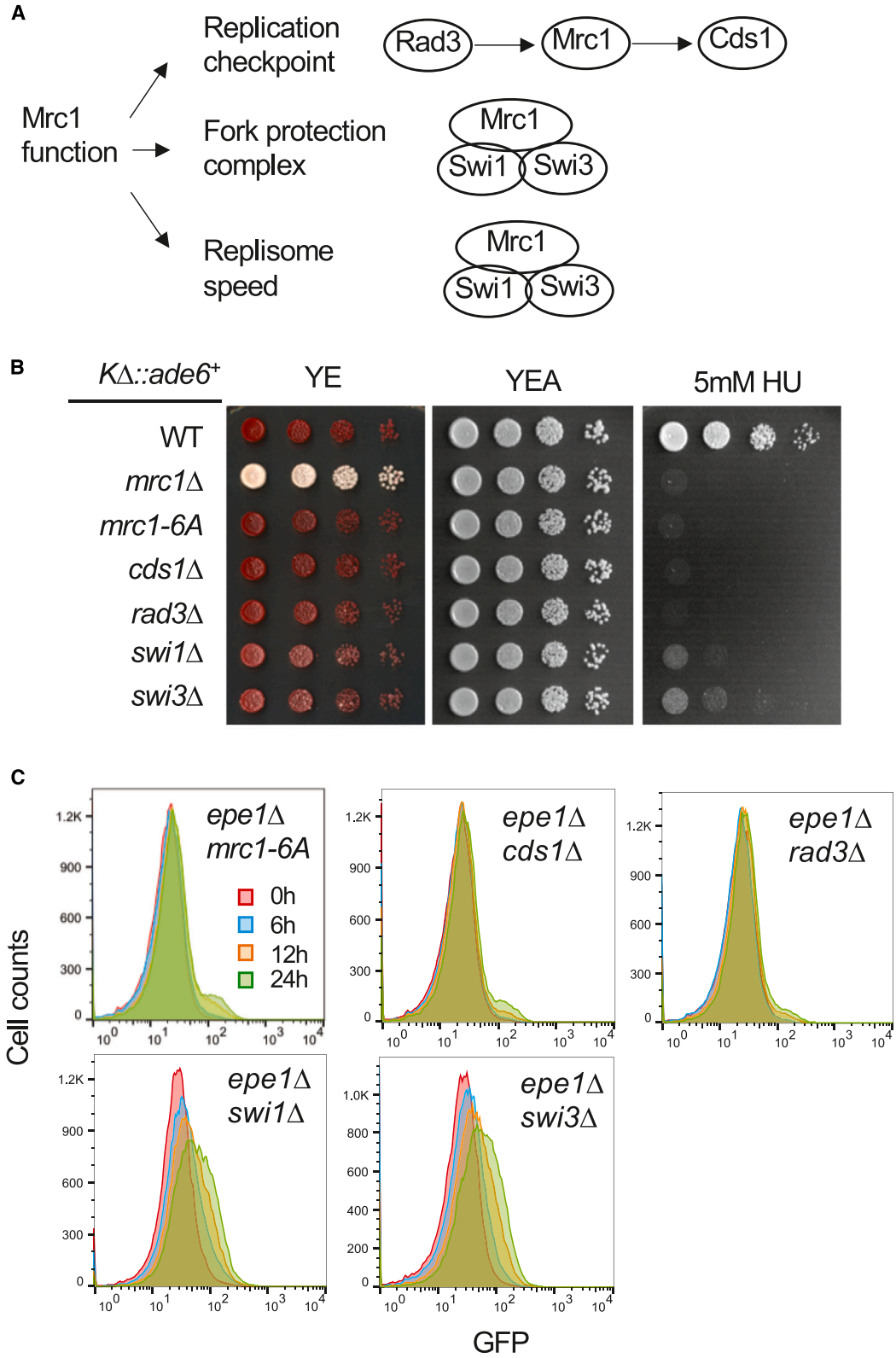

Figure 4. Mrc1 regulates epigenetic inheritance independent of its known roles in DNA replication

(A) Schematic diagram of Mrc1 functions.

(B) Serial dilution analysis of indicated strains to measure the expression of *KΔ::ade6*$^{+}$.

(C) Flow cytometry analysis of GFP expression at different time points after tetracycline addition.

Please cite this article in press as: Toda et al., Mrc1 regulates parental histone segregation and heterochromatin inheritance, Molecular Cell (2024), https://doi.org/10.1016/j.molcel.2024.07.002

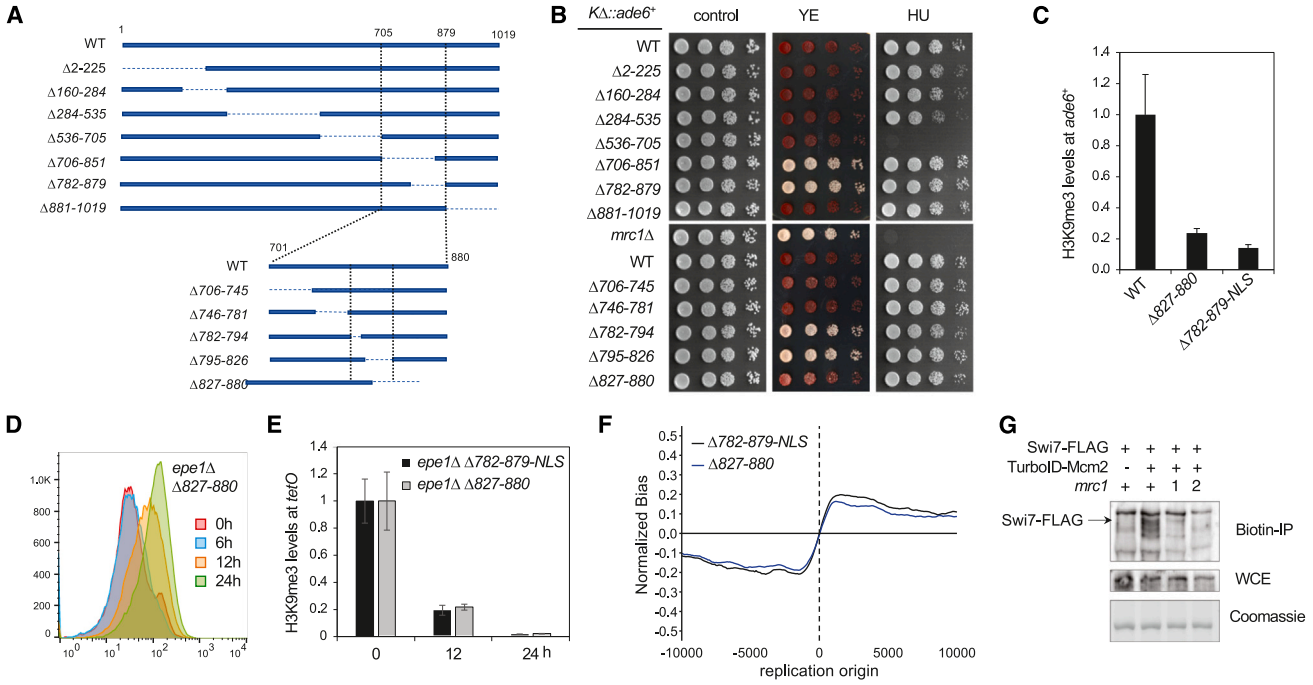

Figure 5. Mapping the region of Mrc1 important for parental histone segregation and epigenetic inheritance

(A) Diagram of Mrc1 truncations and mutations.

(B) Serial dilution analysis of indicated strains to measure the expression of *KΔ::ade6*$^+$ and sensitivity to 5 mM HU.

(C) ChIP analysis of H3K9me3 level at the *KΔ::ade6*$^+$, normalized to *act1*$^+$. Data are presented as mean ± SD of three technical replicates.

(D) Flow cytometry analysis of GFP expression at different time points after tetracycline addition.

(E) ChIP analysis of H3K9me3 level at *tetO*, normalized to *act1*$^+$. Data are presented as mean ± SD of three technical replicates.

(F) eSPAN analysis of H3K4me3 bias levels at replication origins.

(G) Top, western blot analysis of Strep-Tactin purified fractions with a FLAG antibody. Middle, western blot analysis of whole-cell extract (WCE) with a FLAG antibody. Bottom, Coomassie blue stain of Strep-Tactin purified fractions. 1, *Δ827-880*; 2, *Δ782-879-NLS*.

See also Figures S2–S4.

(Figure 5A). Two mutants, *Δ706-851* and *Δ782-879*, are defective in the silencing of *KΔ::ade6*$^+$, although not sensitive to HU (Figure 5B, top). By contrast, the *Δ563-705* mutant, which removes Rad3 phosphorylation sites, is highly sensitive to HU but does not affect *KΔ::ade6*$^+$ silencing (Figure 5B, top). These results further confirm that the role of Mrc1 in regulating heterochromatin inheritance can be separated from its role in regulating the DNA replication checkpoint.

We then generated smaller truncations between amino acid residues 701 and 880 of Mrc1 at the endogenous *mrc1*$^+$ locus (Figure 5A). Among them, *Δ782-794* and *Δ795-826* result in strong silencing defects of *KΔ::ade6*$^+$, while *Δ827-880* shows slightly weaker silencing defects, as indicated colony color on YE medium (Figure 5B, middle). None of these mutations are sensitive to HU, supporting the notion that this region is not involved in DNA replication checkpoint function. Furthermore, western blot analysis confirmed the proper expression of these mutants (Figure S2).

Given the strong phenotypes of *Δ782-794* and *Δ795-826* in heterochromatin inheritance, we generated point mutations of conserved residues within these two regions. Mutations of two positively charged patches to alanines, such as *784-788A* and *806-811A* (Figure S3A), lead to defective silencing of *KΔ::ade6*$^+$ and the inheritance of silenced *tetO-gfp*$^+$ after TetR-Clr4-I in an *epe1Δ* background (Figures S3B–S3E). Moreover, eSPAN analysis of H3K4me3-containing parental histones in these mutants revealed a pronounced bias toward the leading strand for both mutants (Figure S3F). Finally, mass spectrometry and western blot analysis of TurID-Mcm2 biotinylated proteins found that both mutations reduced interaction between Mcm2-HBD and Swi7 but increased interaction between Mcm2-HBD and Cdc45 (Table S2; Figures S3G–S3I).

Immunofluorescence analyses show that both the *784-788A* and *806-811A* mutants reduce the nuclear staining of Mrc1 (Figure S4A), suggesting that these regions are nuclear localization signals (NLSs). Consistent with this idea, the addition of the SV40 T-antigen at the C terminus of Mrc1 in different mutants alleviated the silencing defects of *KΔ::ade6*$^+$ and the inheritance defects of *tetO-gfp*$^+$ in an *epe1Δ* background for *784-788A*, *806-811A*, *Δ782-794*, and *Δ795-826*, but not *Δ706-851* and *Δ782-879* mutants (Figures S4B and S4C). ChIP analyses show that *Δ782-879-NLS* and *Δ827-880* result in a strong decrease of H3K9me3 levels at *KΔ::ade6*$^+$ and rapid loss of H3K9me3 at *tetO* (Figures 5C–5E). Moreover, these two mutations result in strong leading-strand H3K4me3 eSPAN bias (Figure 5F). Additionally, both mutations affect the biotinylation of Swi7 by

Please cite this article in press as: Toda et al., Mrc1 regulates parental histone segregation and heterochromatin inheritance, Molecular Cell (2024), https://doi.org/10.1016/j.molcel.2024.07.002

CellPress

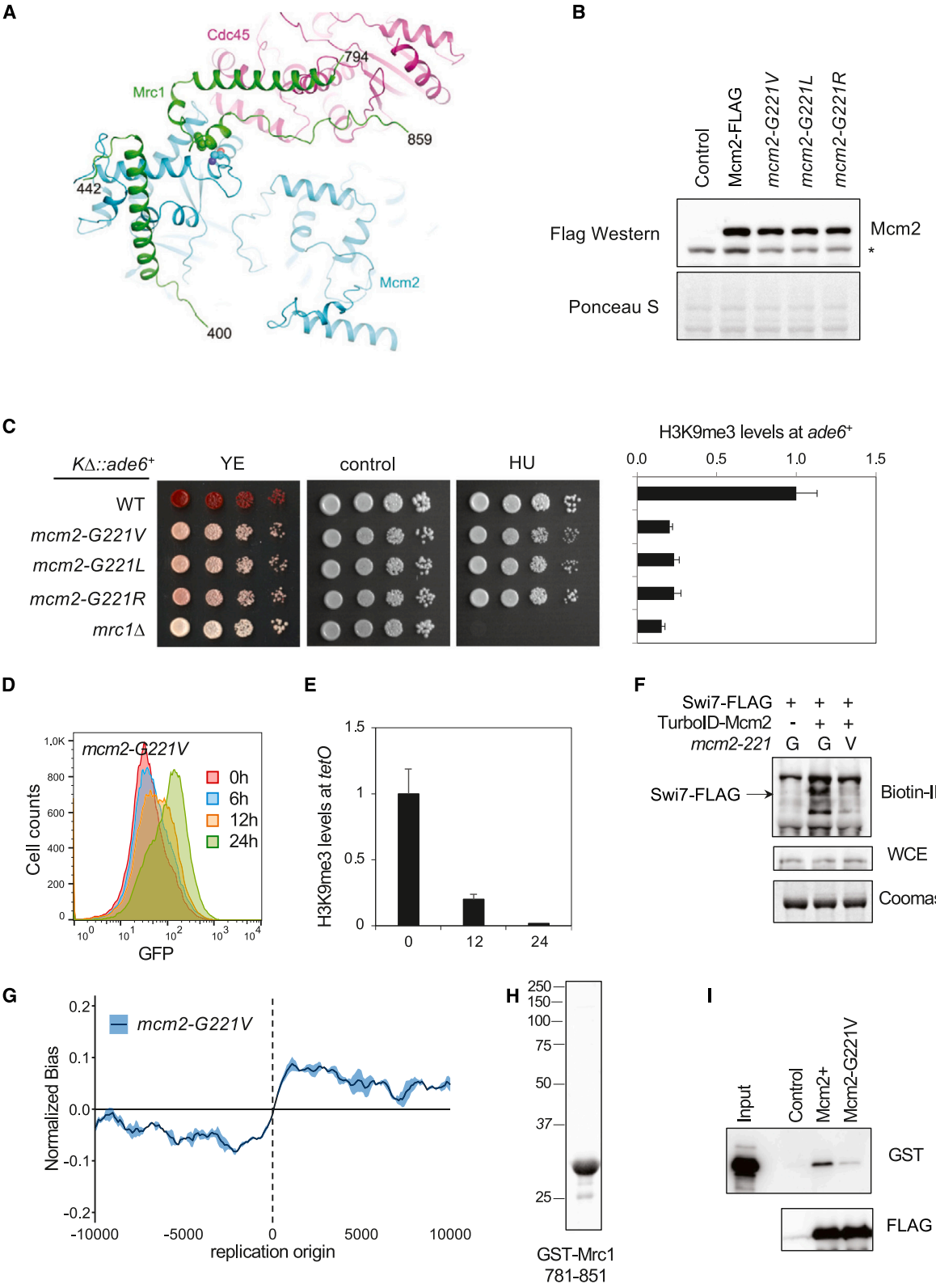

(legend on next page)

Please cite this article in press as: Toda et al., Mrc1 regulates parental histone segregation and heterochromatin inheritance, Molecular Cell (2024), https://doi.org/10.1016/j.molcel.2024.07.002

TurboID-Mcm2 (Figure 5G). These results suggest that residues between 827–879 are critical for Mrc1 function in heterochromatin inheritance and parental histone H3-H4 segregation.

The Mrc1-Mcm2 interaction is critical for parental histone transfer and epigenetic inheritance

We then investigated whether Mrc1 interacts with components of the replisome using AlphaFold Multimer. Interestingly, we found that the 794–859 region of Mrc1 interacts with Mcm2 and Cdc45 (Figures 6A and S5). The predicted interaction between Mcm2 and Cdc45 is consistent with structural studies.[14,16,37] Notably, K205 of Mcm2 and V826 of Mrc1 are in proximity (Figure 6A), aligning well with cross-linking mass spectrometry analysis of the budding yeast replisome.[16] These results suggest that the predicted structure is likely physiologically relevant.

The predicted structure reveals extensive contacts between Mrc1, Mcm2, and Cdc45 (Figures 6A and S5). Importantly, F835 of Mrc1 is inserted within a hydrophobic pocket of Mcm2. We generated the F835A mutation at the endogenous *mrc1*$^+$ locus. Although this mutation leads to a leading-strand H3K4me3 eSPAN bias (Figure S6A), it causes mild silencing defects of *KΔ::ade6*$^+$ and the inheritance of *tetO-gfp*$^+$ in an *epe1Δ* background (Figures S6B and S6C). We reasoned that the milder effect could be due to regions of Mrc1 adjacent to F835 still interacting with Mcm2 and Cdc45, which are not fully disrupted by the F835A mutation. The hydrophobic pocket of Mcm2 that Mrc1-F835 inserts into has a G221 residue at the bottom (Figure S5B). We hypothesized that changing G221 into amino acid residues with larger side chains might have more pronounced effects on the Mrc1-Mcm2 interaction than the Mrc1-F835A mutation. We introduced the G221V, G221L, or G221R mutations at the endogenous *mcm2*$^+$ locus. Western blot analysis indicates that all three mutations are expressed at similar levels to wild-type Mcm2 (Figure 6B). Interestingly, all three mutations lead to defective silencing of *KΔ::ade6*$^+$ as indicated by pink colonies on YE medium and loss of H3K9me3 at the reporter (Figure 6C). In addition, *epe1Δ mcm2-G221V* is defective in the inheritance of *tetO-gfp*$^+$, accompanied by rapid loss of H3K9me3 (Figures 6D and 6E). Moreover, the *mcm2-G221V mrc1-F835A* double mutant behaves similarly to *mcm2-G221V* in the silencing of *KΔ::ade6*$^+$ and the inheritance of *tetO-gfp*$^+$ in an *epe1Δ* background (Figures S5B and S5C). By contrast, *mcm2-G221V* has a mild effect on the silencing of *otr::ade6*$^+$ or H3K9me3 levels at *dh* repeats, similar to *mrc1Δ* (Figures S7A). Furthermore, *mcm2-G221V* blocks the biotinylation of Swi7 by TurboID-Mcm2 (Figure 6F) and results in a leading-strand H3K4me3 eSPAN bias (Figure 6G). These results suggest a crucial role of Mcm2-Mrc1 interaction in parental histone H3-H4 transfer.

We subsequently tested whether the G221V mutation indeed affects the interaction between Mcm2 and Mrc1. Although we obtained highly purified recombinant GST-Mrc1-781-851 from *E. coli* (Figure 6H), purification of Mcm2 fragments was challenging, possibly due to Mcm2 normally exists within the Mcm2-7 complex. Therefore, we affinity-purified the Mcm2-7 complex from cells expressing Mcm2-FLAG or Mcm2-G221V-FLAG. Western blot analysis with a FLAG antibody demonstrates effective purification of Mcm2 (Figure 6I). Consistent with structural predictions, we found that GST-Mrc1-781-851 interacts with the wild-type Mcm2-7 complex but not the Mcm2-7 complex containing Mcm2-G221V (Figure 6I). In addition, mass spectrometry analysis of TurboID-Mcm2-G221V indicates that there are no major changes in the biotinylation of the MCM complex and there is a reduction of Mrc1 biotinylation (Figure S7B; Table S3).

Altogether, these results suggest that Mrc1 interacts with Mcm2, and the interaction is critical for symmetrical parental histone segregation and heterochromatin inheritance.

DISCUSSION

One of the central questions in chromatin-based epigenetic inheritance is how parental histones are distributed to daughter strands, acting as seeds to reinstate parental histone modification patterns. The histone-binding activities of Mcm2 and Pol alpha are responsible for distributing parental histone H3-H4 tetramers to the lagging strands.[6,8,13] However, how the leading strand-associated Mcm2 promotes parental histone transfer to the lagging strand remains unclear.

A major challenge in elucidating the mechanism of parental histone transfer is the lack of assays to perform genetic screens for additional regulators of this process. We have recently shown that in fission yeast, an *mcm2-2A* mutation leads to strong silencing defects of reporter genes, such as *KΔ::ade6*$^+$ and *tetO-gfp*$^+$, which specifically measure heterochromatin

Figure 6. Mrc1-Mcm2 interaction is critical for parental histone segregation and heterochromatin inheritance

(A) AlphaFold Multimer predicted structure of Mrc1 in complex with Mcm2 and Cdc45. The positions of Mrc1-F835 and Mcm2-G221 are indicated as spheres.
(B) Top, western blot analysis of Mcm2-FLAG protein levels. Bottom, Ponceau S stain of the membrane to show total proteins. * represents a non-specific band.
(C) Left, serial dilution analysis of indicated strains to measure the expression of *KΔ::ade6*$^+$. Right, ChIP analysis of H3K9me3 level at the *KΔ::ade6*$^+$, normalized to *act1*$^+$. Data are presented as mean ± SD of three technical replicates.
(D) Flow cytometry analysis of GFP expression at different time points after tetracycline addition. The strain used is in an *epe1Δ* background.
(E) ChIP analysis of H3K9me3 level at *tetO*, normalized to *act1*$^+$. Data are presented as mean ± SD of three technical replicates. The strains used are in an *epe1Δ* background.
(F) Top, western blot analysis of Strep-Tactin purified fractions with a FLAG antibody. Middle, western blot analysis of whole-cell extract (WCE) with a FLAG antibody. Bottom, Coomassie blue stain of Strep-Tactin purified fractions.
(G) eSPAN analysis of H3K4me3 bias levels at replication origins. The shading of the bias line plot is the 95% confidence interval of the mean value of at least two biological replicates, which is about mean ± 2 folds of the standard error.
(H) SDS-PAGE of purified recombinant GST-Mrc1-781-851, and the gel was stained with Coomassie blue.
(I) Western blot analysis of FLAG-Mcm2 associated fractions with a GST antibody (top) and a FLAG antibody (bottom).
See also Figures S5–S7.

Please cite this article in press as: Toda et al., Mrc1 regulates parental histone segregation and heterochromatin inheritance, Molecular Cell (2024), https://doi.org/10.1016/j.molcel.2024.07.002

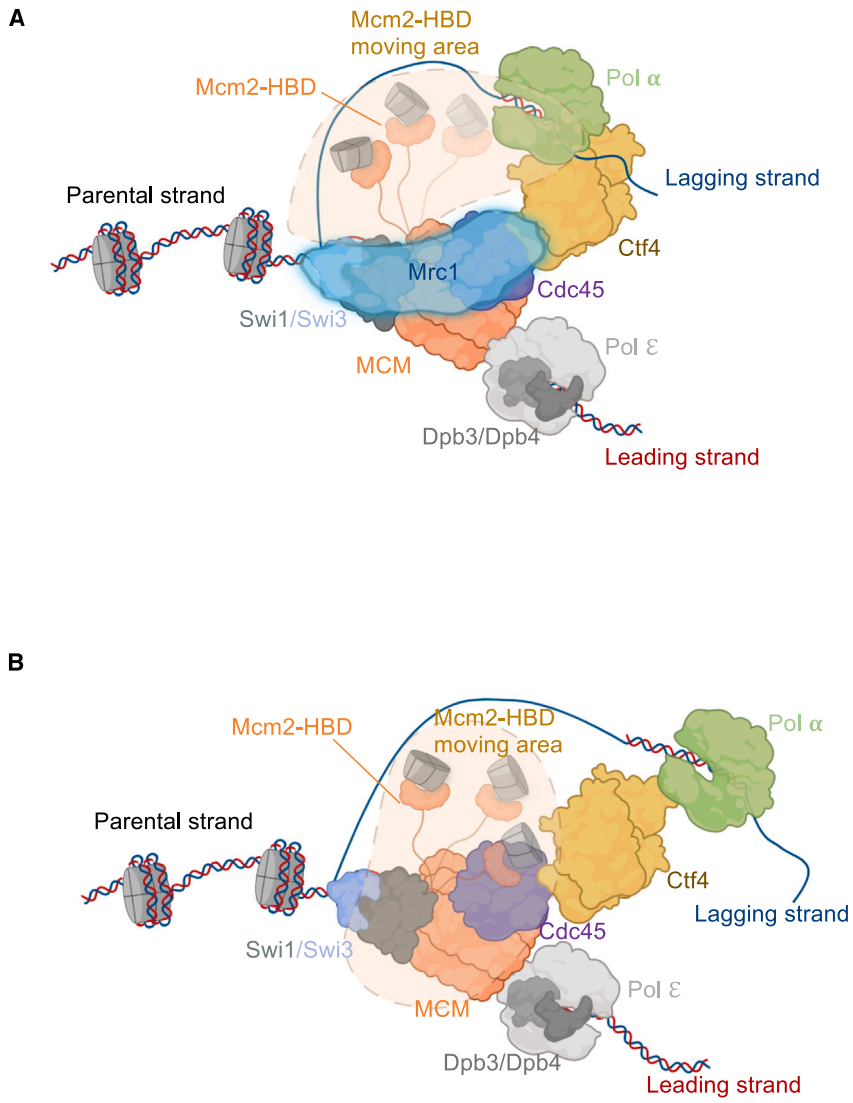

Figure 7. A model for Mrc1's function in parental histone transfer

(A) In wild-type cells, the Mcm2-HBD captures parental histones released at the front of the replication fork and migrates toward the back of the replisome. Mrc1, which covers extensive surface areas of the replisome, directs the movement of Mcm2-HBD along the lagging strand, facilitating the delivery of parental histones to the downstream histone-binding protein Swi7.

(B) In *mrc1* mutant cells, Mcm2-HBD's movement is less restricted and diverted to alternative trajectories. Consequently, the efficient delivery of parental histones from Mcm2-HBD to Swi7 is compromised.

inheritance.[26] Here, we used the *KΔ::ade6*$^{+}$ reporter to screen the fission yeast deletion library for mutations affecting heterochromatin inheritance. In addition to known mutations of heterochromatin regulators, we also identified *mrc1Δ*. Importantly, *mrc1Δ* results in a strong leading-strand H3K4me3 eSPAN bias, suggesting that Mrc1 is required for the deposition of parental histones to the lagging strand.

Mrc1 plays distinct roles in DNA replication by controlling replication speed as well as protecting the replication fork under replication stress. Although the mechanism by which Mrc1 executes such diverse functions remains elusive, our genetic analysis and systematic mapping of Mrc1 regions responsible for heterochromatin inheritance underscores that Mrc1's involvement in parental histone segregation can be disentangled from these recognized roles.

Importantly, our mutational analyses reveal that residues between 782–879 of Mrc1 are critical for heterochromatin inheritance and parental histone segregation, although this region contains two positively charged short segments that act as NLSs. Interestingly, structural predictions by AlphaFold Multimer indicate that the region between 794–859 forms extensive interactions with Mcm2 and Cdc45 near the Mcm2-Cdc45 interface, with F835 of Mrc1 inserting into a hydrophobic pocket of Mcm2 (Figure 6A). The prediction is consistent with cryo-EM data regarding the position of this region Mrc1 within the replisome as well as peptides of Mcm2 and Mrc1 identified by cross-linking mass spectrometry of the replisome.[16] It is also consistent with our mutational analysis indicating that multiple regions within 706–879 might have additive effects on heterochromatin inheritance. For example, the *F835A* and *Δ827-880* mutations of Mrc1 have weaker effects than *Δ782-879-NLS*. We also mutated Mcm2-G221 to amino acids with longer side chains, which is also expected to disrupt the interaction interface between Mcm2 and Mrc1. Interestingly, the mutations lead to heterochromatin inheritance and parental histone segregation defects, corroborating the idea that the Mcm2-Mrc1 interaction interface is critical for parental histone deposition to the lagging strand. Importantly, Mcm2-G221 mutations are viable and not sensitive to HU, suggesting that the mutations maintain the normal function of Mcm2 in DNA replication. It is also interesting to note that the Mcm2-HBD extends out from the Mcm2-7 complex very close to the Mcm2-Cdc45-Mrc1 interface, which occupies an important position to direct the path of Mcm2-HBD (Figure 7A). These results suggest that Mcm2-Mrc1 interaction is critical for parental histone segregation and heterochromatin inheritance.

Our TurboID experiments reveal that Mcm2 can reach the vicinity of Swi7 and that Mrc1 is important for keeping Mcm2 and Swi7 in proximity. Interestingly, TurboID experiments also show stronger biotinylation of Cdc45 by TurboID-Mcm2 in *mrc1* mutant cells, suggesting that Mcm2-HBD is in closer proximity to Cdc45 in the absence of Mrc1. Given the expected

Please cite this article in press as: Toda et al., Mrc1 regulates parental histone segregation and heterochromatin inheritance, Molecular Cell (2024), https://doi.org/10.1016/j.molcel.2024.07.002

position of Mrc1 on the replisome, it likely creates a physical barrier to separate leading and lagging strand parental histone segregation pathways and directs Mcm2-HBD to be close to Swi7 to transfer parental histones to the lagging strand Figure 7A). In the absence of Mrc1, Mcm2-HBD become more flexible spatially and deviates from its normal path, lowering its chance of getting close to Swi7, thus leading to defects in parental histone transfer to the lagging strand (Figure 7B).

It remains unclear how parental histones released from the front of the replisome traverse to their anticipated deposition site at the back of the replisome. Therefore, it is highly plausible that additional histone-binding proteins might be involved to facilitate the relay of parental histones from Mcm2 and Swi7 to the deposition site on lagging strand DNA. It is interesting to note that a separate study also identifies a region within Mrc1 that binds histone H3-H4 tetramers, and mutations of key residues required for histone interaction lead to heterochromatin inheritance defects.[45] Interestingly, the histone-binding mutant of Mrc1 results in little parental histone deposition bias but reduces parental histone levels on both strands. Therefore, Mrc1 seems to be a central hub and performs two distinct functions in regulating parental histone segregation bias and density, and the Mrc1-Mcm2 interaction is important for the symmetrical distribution of parental histones.

The inheritance-specific reporters provide sensitive assays for screening mutations that affect parental histone segregation. Given the essential nature of the core DNA replication machinery, it is not surprising that Mrc1 is the sole component of the replisome identified in our study. Nevertheless, future mutagenesis studies directed at replisome constituents could potentially unveil additional regulators of parental histone segregation, which has been so far eluding genetic screens.

Limitations of the study

Although our study provides clear evidence that Mrc1 regulates parental histone segregation bias and epigenetic inheritance, it also has limitations. For example, in our eSPAN analyses, we used H3K4me3 as a marker for parental histones due to its higher abundance around replication origins. However, heterochromatin regions are enriched for H3K9me3 and depleted for H3K4me3. Although histone chaperones such as Mcm2 interact with the core of histones rather than their tails, suggesting the interaction is likely independent of modifications, it remains possible that the segregation pattern of parental histones containing H3K9me3 differs from those containing H3K4me3.

It is also important to note that TurboID is designed to detect changes in protein-protein proximity rather than direct interactions. Consequently, the apparent proximity between Mcm2 and Swi7 might arise from other interactions within the replisome, not necessarily indicating a direct interaction between the two. Nonetheless, our data indicates that Mcm2 makes less contact with Swi7 in the absence of Mrc1 either spatially or temporally, consistent with defective transfer of parental histones from Mcm2 to Pol alpha. Further analysis to explore histone chaperone-replisome interactions may reveal critical insights into the passage of parental histones from the front to the back of the replisome.

We have not examined whether the Mcm2-G221V or Mrc1-F835A mutations affect the interaction between Mcm2 and Mrc1 *in vivo* by co-immunoprecipitation. This is because Mrc1 has an extensive interaction interface with the replisome. Therefore, these mutations are expected to affect the Mcm2-Mrc1 interaction only locally. Consequently, we do not expect these changes to be detectable by co-immunoprecipitation analysis. However, our mass spectrometry analysis of biotinylated proteins from TurobID-Mcm2-G221V cells shows a reduction of Mrc1 compared with TurboID-Mcm2, which is consistent with a reduction of Mcm2-Mrc1 interaction. Additionally, heterochromatin inheritance and eSPAN analyses strongly suggest that this interaction has functional consequences *in vivo*.

STAR★METHODS

Detailed methods are provided in the online version of this paper and include the following:

- KEY RESOURCES TABLE
- RESOURCE AVAILABILITY
  - Lead contact
  - Materials availability
  - Data and code availability
- EXPERIMENTAL MODEL AND STUDY PARTICIPANT DETAILS
  - Fission yeast strains and genetic analyses
- METHOD DETAILS
  - Flow cytometry
  - Chromatin immunoprecipitation
  - eSPAN
  - Sequencing data analysis
  - TurboID purification
  - Western blot analysis
  - Mass spectrometry analysis
  - AlphaFold calculations
  - Protein-protein interaction assay
- QUANTIFICATION AND STATISTICAL ANALYSIS

SUPPLEMENTAL INFORMATION

Supplemental information can be found online at https://doi.org/10.1016/j.molcel.2024.07.002.

ACKNOWLEDGMENTS

We thank Ke Zhang, Kaushik Ragunathan, Paul Russell, Susan Forsburg, Nick Rhind, and Francois Bachand for yeast strains. This work was supported by NIH grants R35GM126910 to S.J.; R35GM118015 to Z.Z.; R35GM149572 to F.Q.; R35GM118093 to L.T.; and R35GM128802, R01AG071869, R01AG071869, and R01HG012216 to M.J. as well as NSF grant 2224211 to M.J. and NSF Graduate Research Fellowships Program grant DGE2035197 to L.C.T.

AUTHOR CONTRIBUTIONS

S.J. and C.-M.S. conceived the project. S.J., C.-M.S., and L.T. designed experiments. T.T., S.J., Y.F., C.-M.S., J.-K.K., and L.C.T. performed experiments. X.H. performed eSPAN analysis. L.T. performed AlphaFold Multimer prediction. S.J., Z.Z., F.Q., L.T., and M.J. supervised the research. S.J. and T.T. wrote the manuscript with input from all authors.

DECLARATION OF INTERESTS

The authors declare no competing interests.

DECLARATION OF GENERATIVE AI AND AI-ASSISTED TECHNOLOGIES IN THE WRITING PROCESS

During the preparation of this work, the authors used ChatGPT to improve language and readability. After using this tool/service, the authors reviewed and edited the content as needed and take full responsibility for the content of the publication.

Received: October 19, 2023
Revised: June 7, 2024
Accepted: July 3, 2024
Published: August 1, 2024

REFERENCES

1. Du, W., Shi, G., Shan, C.M., Li, Z., Zhu, B., Jia, S., Li, Q., and Zhang, Z. (2022). Mechanisms of chromatin-based epigenetic inheritance. Sci. China Life Sci. *65*, 2162–2190. https://doi.org/10.1007/s11427-022-2120-1.
2. Escobar, T.M., Loyola, A., and Reinberg, D. (2021). Parental nucleosome segregation and the inheritance of cellular identity. Nat. Rev. Genet. *22*, 379–392. https://doi.org/10.1038/s41576-020-00312-w.
3. Schlissel, G., and Rine, J. (2019). The nucleosome core particle remembers its position through DNA replication and RNA transcription. Proc. Natl. Acad. Sci. USA *116*, 20605–20611. https://doi.org/10.1073/pnas.1911943116.
4. Escobar, T.M., Oksuz, O., Saldaña-Meyer, R., Descostes, N., Bonasio, R., and Reinberg, D. (2019). Active and Repressed Chromatin Domains Exhibit Distinct Nucleosome Segregation during DNA Replication. Cell *179*, 953–963.e11. https://doi.org/10.1016/j.cell.2019.10.009.
5. Xu, M., Long, C., Chen, X., Huang, C., Chen, S., and Zhu, B. (2010). Partitioning of histone H3-H4 tetramers during DNA replication-dependent chromatin assembly. Science *328*, 94–98. https://doi.org/10.1126/science.1178994.
6. Yu, C., Gan, H., Serra-Cardona, A., Zhang, L., Gan, S., Sharma, S., Johansson, E., Chabes, A., Xu, R.M., and Zhang, Z. (2018). A mechanism for preventing asymmetric histone segregation onto replicating DNA strands. Science *361*, 1386–1389. https://doi.org/10.1126/science.aat8849.
7. Gan, H., Serra-Cardona, A., Hua, X., Zhou, H., Labib, K., Yu, C., and Zhang, Z. (2018). The Mcm2-Ctf4-Polalpha Axis Facilitates Parental Histone H3-H4 Transfer to Lagging Strands. Mol. Cell *72*, 140–151.e3. https://doi.org/10.1016/j.molcel.2018.09.001.
8. Petryk, N., Dalby, M., Wenger, A., Stromme, C.B., Strandsby, A., Andersson, R., and Groth, A. (2018). MCM2 promotes symmetric inheritance of modified histones during DNA replication. Science *361*, 1389–1392. https://doi.org/10.1126/science.aau0294.
9. Zhang, K., Mosch, K., Fischle, W., and Grewal, S.I.S. (2008). Roles of the Clr4 methyltransferase complex in nucleation, spreading and maintenance of heterochromatin. Nat. Struct. Mol. Biol. *15*, 381–388. https://doi.org/10.1038/nsmb.1406.
10. Nakayama, J., Rice, J.C., Strahl, B.D., Allis, C.D., and Grewal, S.I. (2001). Role of histone H3 lysine 9 methylation in epigenetic control of heterochromatin assembly. Science *292*, 110–113. https://doi.org/10.1126/science.1060118.
11. Rea, S., Eisenhaber, F., O'Carroll, D., Strahl, B.D., Sun, Z.W., Schmid, M., Opravil, S., Mechtler, K., Ponting, C.P., Allis, C.D., and Jenuwein, T. (2000). Regulation of chromatin structure by site-specific histone H3 methyltransferases. Nature *406*, 593–599. https://doi.org/10.1038/35020506.
12. Jih, G., Iglesias, N., Currie, M.A., Bhanu, N.V., Paulo, J.A., Gygi, S.P., Garcia, B.A., and Moazed, D. (2017). Unique roles for histone H3K9me states in RNAi and heritable silencing of transcription. Nature *547*, 463–467. https://doi.org/10.1038/nature23267.
13. Li, Z., Hua, X., Serra-Cardona, A., Xu, X., Gan, S., Zhou, H., Yang, W.S., Chen, C.L., Xu, R.M., and Zhang, Z. (2020). DNA polymerase alpha interacts with H3-H4 and facilitates the transfer of parental histones to lagging strands. Sci. Adv. *6*, eabb5820. https://doi.org/10.1126/sciadv.abb5820.
14. Jones, M.L., Baris, Y., Taylor, M.R.G., and Yeeles, J.T.P. (2021). Structure of a human replisome shows the organisation and interactions of a DNA replication machine. EMBO J. *40*, e108819. https://doi.org/10.15252/embj.2021108819.
15. Yuan, Z., Georgescu, R., Schauer, G.D., O'Donnell, M.E., and Li, H. (2020). Structure of the polymerase epsilon holoenzyme and atomic model of the leading strand replisome. Nat. Commun. *11*, 3156. https://doi.org/10.1038/s41467-020-16910-5.
16. Baretić, D., Jenkyn-Bedford, M., Aria, V., Cannone, G., Skehel, M., and Yeeles, J.T.P. (2020). Cryo-EM Structure of the Fork Protection Complex Bound to CMG at a Replication Fork. Mol. Cell *78*, 926–940.e13. https://doi.org/10.1016/j.molcel.2020.04.012.
17. Yu, C., Gan, H., Han, J., Zhou, Z.X., Jia, S., Chabes, A., Farrugia, G., Ordog, T., and Zhang, Z. (2014). Strand-specific analysis shows protein binding at replication forks and PCNA unloading from lagging strands when forks stall. Mol. Cell *56*, 551–563. https://doi.org/10.1016/j.molcel.2014.09.017.
18. Shan, C.M., Fang, Y., and Jia, S. (2023). Leaving histone unturned for epigenetic inheritance. FEBS Journal *290*, 310–320. https://doi.org/10.1111/febs.16260.
19. Grewal, S.I.S. (2023). The molecular basis of heterochromatin assembly and epigenetic inheritance. Mol. Cell *83*, 1767–1785. https://doi.org/10.1016/j.molcel.2023.04.020.
20. Allshire, R.C., and Madhani, H.D. (2018). Ten principles of heterochromatin formation and function. Nat. Rev. Mol. Cell Biol. *19*, 229–244. https://doi.org/10.1038/nrm.2017.119.
21. Moazed, D. (2011). Mechanisms for the inheritance of chromatin states. Cell *146*, 510–518. https://doi.org/10.1016/j.cell.2011.07.013.
22. Hall, I.M., Shankaranarayana, G.D., Noma, K.I., Ayoub, N., Cohen, A., and Grewal, S.I.S. (2002). Establishment and maintenance of a heterochromatin domain. Science *297*, 2232–2237. https://doi.org/10.1126/science.1076466.
23. Grewal, S.I., and Klar, A.J. (1996). Chromosomal inheritance of epigenetic states in fission yeast during mitosis and meiosis. Cell *86*, 95–101.
24. Ragunathan, K., Jih, G., and Moazed, D. (2015). Epigenetics. Epigenetic inheritance uncoupled from sequence-specific recruitment. Science *348*, 1258699. https://doi.org/10.1126/science.1258699.
25. Audergon, P.N.C.B., Catania, S., Kagansky, A., Tong, P., Shukla, M., Pidoux, A.L., and Allshire, R.C. (2015). Epigenetics. Restricted epigenetic inheritance of H3K9 methylation. Science *348*, 132–135. https://doi.org/10.1126/science.1260638.
26. Fang, Y., Hua, X., Shan, C.M., Toda, T., Qiao, F., Zhang, Z., and Jia, S. (2024). Coordination of histone chaperones for parental histone segregation and epigenetic inheritance. Genes Dev. *38*, 189–204. https://doi.org/10.1101/gad.351278.123.
27. Smits, V.A.J., Cabrera, E., Freire, R., and Gillespie, D.A. (2019). Claspin - checkpoint adaptor and DNA replication factor. FEBS Journal *286*, 441–455. https://doi.org/10.1111/febs.14594.
28. Shipkovenska, G., Durango, A., Kalocsay, M., Gygi, S.P., and Moazed, D. (2020). A conserved RNA degradation complex required for spreading and epigenetic inheritance of heterochromatin. eLife *9*, e54341. https://doi.org/10.7554/eLife.54341.
29. Volpe, T.A., Kidner, C., Hall, I.M., Teng, G., Grewal, S.I.S., and Martienssen, R.A. (2002). Regulation of heterochromatic silencing and histone H3 lysine-9 methylation by RNAi. Science *297*, 1833–1837. https://doi.org/10.1126/science.1074973.
30. Verdel, A., Jia, S., Gerber, S., Sugiyama, T., Gygi, S., Grewal, S.I.S., and Moazed, D. (2004). RNAi-mediated targeting of heterochromatin by the

RITS complex. Science *303*, 672–676. https://doi.org/10.1126/science.1093686.

31. Huang, H., Strømme, C.B., Saredi, G., Hödl, M., Strandsby, A., González-Aguilera, C., Chen, S., Groth, A., and Patel, D.J. (2015). A unique binding mode enables MCM2 to chaperone histones H3-H4 at replication forks. Nat. Struct. Mol. Biol. *22*, 618–626. https://doi.org/10.1038/nsmb.3055.
32. Foltman, M., Evrin, C., De Piccoli, G., Jones, R.C., Edmondson, R.D., Katou, Y., Nakato, R., Shirahige, K., and Labib, K. (2013). Eukaryotic replisome components cooperate to process histones during chromosome replication. Cell Rep. *3*, 892–904. https://doi.org/10.1016/j.celrep.2013.02.028.
33. Sivakumar, S., Porter-Goff, M., Patel, P.K., Benoit, K., and Rhind, N. (2004). In vivo labeling of fission yeast DNA with thymidine and thymidine analogs. Methods *33*, 213–219. https://doi.org/10.1016/j.ymeth.2003.11.016.
34. Hodson, J.A., Bailis, J.M., and Forsburg, S.L. (2003). Efficient labeling of fission yeast Schizosaccharomyces pombe with thymidine and BUdR. Nucleic Acids Res. *31*, e134. https://doi.org/10.1093/nar/gng134.
35. Larochelle, M., Bergeron, D., Arcand, B., and Bachand, F. (2019). Proximity-dependent biotinylation mediated by TurboID to identify protein-protein interaction networks in yeast. J. Cell Sci. *132*, jcs232249. https://doi.org/10.1242/jcs.232249.
36. Liu, Q., Greimann, J.C., and Lima, C.D. (2006). Reconstitution, activities, and structure of the eukaryotic RNA exosome. Cell *127*, 1223–1237. https://doi.org/10.1016/j.cell.2006.10.037.
37. Jones, M.L., Aria, V., Baris, Y., and Yeeles, J.T.P. (2023). How Pol alpha-primase is targeted to replisomes to prime eukaryotic DNA replication. Mol. Cell *83*, 2911–2924.e16. https://doi.org/10.1016/j.molcel.2023.06.035.
38. Evrin, C., Maman, J.D., Diamante, A., Pellegrini, L., and Labib, K. (2018). Histone H2A-H2B binding by Pol alpha in the eukaryotic replisome contributes to the maintenance of repressive chromatin. EMBO J *37*, e99021. https://doi.org/10.15252/embj.201899021.
39. Tanaka, K., and Russell, P. (2001). Mrc1 channels the DNA replication arrest signal to checkpoint kinase Cds1. Nat. Cell Biol. *3*, 966–972. https://doi.org/10.1038/ncb1101-966.
40. Alcasabas, A.A., Osborn, A.J., Bachant, J., Hu, F., Werler, P.J., Bousset, K., Furuya, K., Diffley, J.F., Carr, A.M., and Elledge, S.J. (2001). Mrc1 transduces signals of DNA replication stress to activate Rad53. Nat. Cell Biol. *3*, 958–965. https://doi.org/10.1038/ncb1101-958.
41. Zhao, H., Tanaka, K., Nogochi, E., Nogochi, C., and Russell, P. (2003). Replication checkpoint protein Mrc1 is regulated by Rad3 and Tel1 in fission yeast. Mol. Cell. Biol. *23*, 8395–8403. https://doi.org/10.1128/MCB.23.22.8395-8403.2003.
42. Shyian, M., and Shore, D. (2021). Approaching Protein Barriers: Emerging Mechanisms of Replication Pausing in Eukaryotes. Front. Cell Dev. Biol. *9*, 672510. https://doi.org/10.3389/fcell.2021.672510.
43. Yeeles, J.T.P., Janska, A., Early, A., and Diffley, J.F.X. (2017). How the Eukaryotic Replisome Achieves Rapid and Efficient DNA Replication. Mol. Cell *65*, 105–116. https://doi.org/10.1016/j.molcel.2016.11.017.
44. Noguchi, E., Noguchi, C., McDonald, W.H., Yates, J.R., 3rd, and Russell, P. (2004). Swi1 and Swi3 are components of a replication fork protection complex in fission yeast. Mol. Cell. Biol. *24*, 8342–8355. https://doi.org/10.1128/MCB.24.19.8342-8355.2004.
45. Yu, J., Zhang, Y., Fang, Y., Paulo, J.A., Yaghoubi, D., Hua, X., Shipkovenska, G., Toda, T., Zhang, Z., Gygi, et al. (2024). Mrc1/CLASPIN acts as a parental histone distribution site in the replisome required for heterochromatin inheritance. Cell *187*. https://doi.org/10.1016/j.cell.2024.07.006.
46. Torres-Garcia, S., Di Pompeo, L., Eivers, L., Gaborieau, B., White, S.A., Pidoux, A.L., Kanigowska, P., Yaseen, I., Cai, Y., and Allshire, R.C. (2020). SpEDIT: A fast and efficient CRISPR/Cas9 method for fission yeast. Wellcome Open Res. *5*, 274. https://doi.org/10.12688/wellcomeopenres.16405.1.
47. Langmead, B., and Salzberg, S.L. (2012). Fast gapped-read alignment with Bowtie 2. Nat. Methods *9*, 357–359. https://doi.org/10.1038/nmeth.1923.
48. Tarasov, A., Vilella, A.J., Cuppen, E., Nijman, I.J., and Prins, P. (2015). Sambamba: fast processing of NGS alignment formats. Bioinformatics *31*, 2032–2034. https://doi.org/10.1093/bioinformatics/btv098.
49. Ramírez, F., Ryan, D.P., Grüning, B., Bhardwaj, V., Kilpert, F., Richter, A.S., Heyne, S., Dündar, F., and Manke, T. (2016). deepTools2: a next generation web server for deep-sequencing data analysis. Nucleic Acids Res. *44*, W160–W165. https://doi.org/10.1093/nar/gkw257.
50. Li, Z., Hua, X., Serra-Cardona, A., Xu, X., and Zhang, Z. (2021). Efficient and strand-specific profiling of replicating chromatin with enrichment and sequencing of protein-associated nascent DNA in mammalian cells. Nat. Protoc. *16*, 2698–2721. https://doi.org/10.1038/s41596-021-00520-6.
51. Moggridge, S., Sorensen, P.H., Morin, G.B., and Hughes, C.S. (2018). Extending the Compatibility of the SP3 Paramagnetic Bead Processing Approach for Proteomics. J. Proteome Res. *17*, 1730–1740. https://doi.org/10.1021/acs.jproteome.7b00913.
52. Bruderer, R., Bernhardt, O.M., Gandhi, T., Miladinović, S.M., Cheng, L.Y., Messner, S., Ehrenberger, T., Zanotelli, V., Butscheid, Y., Escher, C., et al. (2015). Extending the limits of quantitative proteome profiling with data-independent acquisition and application to acetaminophen-treated three-dimensional liver microtissues. Mol. Cell. Proteomics *14*, 1400–1410. https://doi.org/10.1074/mcp.M114.044305.
53. Mirdita, M., Schütze, K., Moriwaki, Y., Heo, L., Ovchinnikov, S., and Steinegger, M. (2022). ColabFold: making protein folding accessible to all. Nat. Methods *19*, 679–682. https://doi.org/10.1038/s41592-022-01488-1.
54. Emsley, P., and Cowtan, K. (2004). Coot: model-building tools for molecular graphics. Acta Crystallogr. D Biol. Crystallogr. *60*, 2126–2132. https://doi.org/10.1107/S0907444904019158.

Please cite this article in press as: Toda et al., Mrc1 regulates parental histone segregation and heterochromatin inheritance, Molecular Cell (2024), https://doi.org/10.1016/j.molcel.2024.07.002

STAR★METHODS

KEY RESOURCES TABLE

REAGENT or RESOURCE	SOURCE	IDENTIFIER
Antibodies		
Polyclonal rabbit anti-H3K9me3	Active Motif	Cat# 39161; RRID: AB_2532132
Polyclonal rabbit anti-H3K4me3	Millipore	Cat# 07-473; RRID: AB_1977252
Polyclonal rabbit anti-BrdU	BD bioscience	Cat# 555627; RRID: AB_395993
Polyclonal rabbit anti-c-myc (A14)	Santa Cruz	Cat# sc-789; RRID: AB_631274
Polyclonal rabbit anti-c-myc	Sigma	Cat# C3956; RRID: AB_439680
Monoclonal mouse anti-FLAG	Sigma	Cat# F3165; RRID: AB_259529
Monoclonal mouse anti-GST	Sigma	Cat# G7781; RRID: AB_259965
Chemicals, peptides, and recombinant proteins		
Geneticin (G418)	Gibco	Cat# 11811-098
Nourseothricin Sulfate	Gold Biotechnology	Cat# N-500-1
Hygromycin B	Gold Biotechnology	Cat# H-270-10
Tetracycline	Sigma	Cat# 87128
BrdU	Sigma	Cat# B5002
Hydroxyurea	Sigma	Cat# H8627
Phenol-chloroform-isoamyl alcohol mixture	Sigma	Cat# 77617
Protein G agarose beads	Sigma	Cat# 11243222001
Protein G Sepharose beads	Cytiva	Cat# 17-0618-01
Proteinase K	Invitrogen	Cat# 10005393
Strep-Tactin Sepharose resin	IBA Life Sciences	Cat# 21201002
Glutathione Sepharose 4B	GE healthcare	Cat# 17-0756-01
FLAG-agarose beads	Sigma	Cat# A2220
Critical commercial assays		
Luna Universal qPCR master mix	New England Biolabs	Cat# M3003S
MiniElute PCR purification kit	Qiagen	Cat# 28004
xGen ssDNA and Low-Input DNA library preparation kit	IDT	Cat# 10009817
Deposited data		
Sequencing Data	This paper	GEO: GSE237700
Mass spectrometry data	This paper	MASSive: MSV000092452
Experimental models: Organisms/strains		
S. pombe strains	Table S4	N/A
Fission yeast deletion library	Bioneer	Cat#2030H
Oligonucleotides		
Primers	Table S5	N/A
Software and algorithms		
FlowJo	Becton, Dickinson and Company	v10.6.2
FACSDiva	Becton, Dickinson and Company	v2.1.0

RESOURCE AVAILABILITY

Lead contact

Further information and request for resources and reagents should be directed to and will be fulfilled by the lead contact, songtao.jia@columbia.edu.

Please cite this article in press as: Toda et al., Mrc1 regulates parental histone segregation and heterochromatin inheritance, Molecular Cell (2024), https://doi.org/10.1016/j.molcel.2024.07.002

Materials availability

All unique, stable reagents generated in this study are available form the lead contact.

Data and code availability

- All high-throughput sequencing data have been deposited at NCBI GEO, accession number GSE237700, and all mass spectrometry data have been deposited to MASSive, accession number MSV000092452, and are publicly available as of the date of publication.
- This paper does not report original code.
- Any additional information needed to reanalyze the data reported in this paper is available from the lead contact upon request.

EXPERIMENTAL MODEL AND STUDY PARTICIPANT DETAILS

Fission yeast strains and genetic analyses

Deletion strains, including *mrc1Δ*, were derived from the Bioneer deletion library and the correct gene deletions were confirmed by PCR analysis and sequencing. Mutations in *mrc1*$^{+}$ and *TurboID-mcm2*$^{+}$ were generated through CRISPR-mediated recombination at their respective chromosomal locations.[46] Cdc45-FLAG and Swi7-FLAG were generated by a PCR-based module method. A list of fission yeast strains used in this study is provided in Table S4. For serial dilution analysis, ten-fold dilutions of mid-log stage fission yeast cultures were plated on the specified media and incubated at 30°C for three days.

For the screen with the deletion library, a query strain was constructed by inserting a *natMX6* cassette near *KΔ::ade6*$^{+}$ and a *hphMX6* cassette at the endogenous *ade6-210* mutant allele. Query strain was crossed with a library of strains that contains individual gene deletion marked with a *kanMX6* cassette, using a Singer RoToR HDA pinning robot on SPA medium. Plates were incubated at 25℃ for 3 days, then 42℃ for 3 more days to kill vegetative cells. Strains were then germinated and the correct genotype was selected by pinning to YES+GNH (Geneticin, Nourseothricin, and Hygromycin) medium, and then pinned to YE medium for color readout. Individual candidate gene deletions are also directly tested through genetic crosses.

METHOD DETAILS

Flow cytometry

Fission yeast strains were cultured in YEA medium and maintained at mid-log phase through regular dilution with fresh medium. Cells were collected at specified time points after tetracycline addition (2.5μg/ml), washed with cold PBS (10 mM Na_2HPO_4, 1.8 mM KH_2PO_4, pH 7.4, 137 mM NaCl, 2.7mM KCl), and fixed with 70% ethanol on ice. After two additional washes with PBS, cells were resuspended in a flow cytometry tube (Corning 352008). GFP expression levels were measured using FACSCelesta (Becton Dickinson) with 488 nm excitation. Data collection was performed using Cellquest (Becton Dickinson), and a primary gate based on physical parameters (forward- and side-light scatter) was set to exclude dead cells and debris. Typically, 50,000 cells were analyzed for each strain at each time point. Raw data were processed using FlowJo (10.6.2, Becton Dickinson).

Chromatin immunoprecipitation

Log phase yeast cultures were crosslinked with 1% formaldehyde for 20 minutes at room temperature, followed by the addition of 125 mM glycine for 5 minutes. Cells were then harvested and washed with cold PBS and resuspended in ChIP lysis buffer (50 mM HEPES-KOH, pH 7.5, 140 mM NaCl, 1% Triton X-100, 0.1% Deoxycholate, 1 mM PMSF). Cold glass beads were added, and the mixture was vigorously shaken in a MiniBeadBeater (Biospec Products). The lysates were collected and sonicated with Bioruptor® Pico (Diagenode) for 12 cycles (30 seconds on/30 seconds off). After centrifugation at 1,3000 rpm for 15 minutes to clarify the lysates, released chromatin was immunoprecipitated overnight at 4°C with antibodies: H3K4me3 (EMD Millipore 07-473) and H3K9me3 (Active Motif 39161). Protein G Agarose beads (Sigma 11243233001) were added for an additional 2 hours at 4°C. The beads were washed twice with ChIP lysis buffer, once each with ChIP lysis buffer containing 0.5 M NaCl, Wash buffer (10 mM Tris, pH 8.0, 250 mM LiCl, 0.5% NP-40, 0.5% Deoxycholate, 1 mM EDTA), and TE buffer (50 mM Tris pH 8.0, 1 mM EDTA). Beads-bounded chromatin was eluted with TES buffer (50 mM Tris pH 8.0, 1 mM EDTA, 1% SDS) at 65°C and then incubated overnight at 65°C to reverse crosslinking. The DNA-protein mixtures were treated with Proteinase K (Invitrogen 10005393), and DNA was purified by phenol: chloroform extraction, followed by ethanol precipitation.

Quantitative PCR (qPCR) was performed using Luna Universal qPCR Master Mix (NEB M3003S) on a StepOne Plus Real-Time PCR System (Applied Biosystems). DNA serial dilutions were used as templates to generate a standard curve of amplification for each pair of primers, and the relative concentration of the target sequence was calculated accordingly. An *act1* fragment was used to calculate the enrichment of ChIP over whole cell extract (WCE) for each target sequence. The concentration of each target gene in wild-type cells was arbitrarily set to 1 and served as a reference for other samples. A list of DNA oligos used is provided in Table S5.

Please cite this article in press as: Toda et al., Mrc1 regulates parental histone segregation and heterochromatin inheritance, Molecular Cell (2024), https://doi.org/10.1016/j.molcel.2024.07.002

eSPAN

Yeast strains containing the *cdc25-22* temperature-sensitive mutant were initially grown at the permissive temperature (25°C) until reaching OD 0.2∼0.4. Cells were incubated for 4 hours at 36°C to arrest at the G2 phase of the cell cycle and then shifted back to 25°C to allow for synchronous entry into the S phase. 25 minutes after the temperature shift, BrdU (Sigma-Aldrich B5002) was added to a final concentration of 650 μM. Cells were crosslinked at 60 minutes after temperature shift with the addition of 1% formaldehyde for 20 minutes. Cell lysis and immunoprecipitation were performed as described in ChIP. Crosslinking was reversed by Chelex-100 (Bio-rad 142-1253).

For BrdU IP, total and ChIP DNA were incubated at 100°C and immediately cooled on ice. The DNA was diluted with BrdU IP buffer (PBS with 0.0625% Triton X-100), and incubated with BrdU antibody (BD Bioscience 555627) for two hours at 4°C. Sepharose Protein G beads (Cytiva 17-0618-01) were added and further incubated for one hour at 4°C. The beads were washed three times with BrdU IP buffer and once with TE buffer. DNA was eluted with TES buffer and purified with the QIAGEN MinElute PCR Purification kit (Qiagen 28004). The single-stranded DNA (ssDNA) libraries were prepared using xGen™ ssDNA & Low-Input DNA Library Preparation Kit (IDT 10009817).

Sequencing data analysis

The input, ChIP, BrdU-IP, and eSPAN ssDNA libraries were sequenced by pair-end sequencing under Illumina NextSeq platforms at Columbia University Irving Medical Center supported by Herbert Irving Comprehensive Cancer Center. The raw reads were firstly trimmed by Trim Galore (https://www.bioinformatics.babraham.ac.uk/projects/trim_galore/) to remove adapters and low-quality reads, and then mapped to the *S. pombe* genome using Bowtie2.[47] PCR-duplicated reads were filtered by Sambamba.[48] The genome-wide reads coverage on the Watson- and Crick strands were calculated at the bin of 1bp using deepTools bamCoverage.[49]

The bias of the reads coverage between the Watson and Crick strands was calculated at each bin surrounding the *S. pombe* origins using the formula: Bias= (W−C) / (W+C), where W and C are the reads coverage on the Watson- and Crick strands, respectively. For the calculation of bias, we used the bin of 100bp sliding window in the [-10kb, 10kb] region surrounding the origins using the code from https://github.com/clouds-drift/eSPAN-bias.[50] For each strain, the eSPAN bias and BrdU bias were both calculated. To avoid the background influence from BrdU, the eSPAN bias is further normalized with the corresponding BrdU bias by subtraction.

TurboID purification

Log phase yeast cultures were collected, washed with cold PBS, and resuspended in ChIP lysis buffer. Cold glass beads were added, and the mixture was vigorously shaken in a MiniBeadBeater (Biospec Products). The lysates were collected and sonicated with Bioruptor® Pico (Diagenode) for 12 cycles (30 seconds on/30 seconds off). The cleared lysates were incubated with Step-Tactin Sepharose resin (IBA LifeSciences 21201002) for two hours at 4°C. The beads were washed twice with ChIP lysis buffer, four times with ChIP lysis buffer containing 0.5 M NaCl, twice with Wash buffer, and once with ChIP lysis buffer. Bound proteins were then eluted with ChIP lysis buffer containing 10 mM biotin.

Western blot analysis

Whole cell lysates or proteins eluted from beads were mixed with 2xSDS loading dye and resolved by SDS-PAGE. Western blot analyses were performed with FLAG M2 (Sigma F3165) and c-Myc (Sigma C3956).

Mass spectrometry analysis

Eluted samples were treated with 5 mM dithiothreitol for 45 minutes at room temperature to reduce disulfide bonds, and cysteines were subsequently alkylated with 10 mM iodoacetamide in the dark for 45 minutes at room temperature. Proteins were precipitated onto magnetic SP3 beads[51] by adding ethanol to the samples, resulting in a sample that was 50% organic solvent, and by shaking for 8 minutes at room temperature. Beads were washed 3 times with 80% ethanol and reconstituted in ammonium bicarbonate. Samples were then digested off the beads using Promega sequencing grade modified trypsin in an enzyme-to-substrate ratio of 1:50. After 16 hours of digestion, samples were taken off the magnetic beads, acidified to a final concentration of 1% formic acid, dried down using a Thermo Savant SpeedVac, and reconstituted in 3%Acn/0.2%FA for injection into the MS.

About 1 μg of total peptides were analyzed on a Waters M-Class UPLC using a 25cm IonOpticks Aurora column (75μm inner diameter; 1.7μm particle size; heated to 45°C) coupled to a benchtop Thermo Fisher Scientific Orbitrap Q Exactive HF mass spectrometer. Peptides were separated at a flow rate of 400 nL/min with a 90 min gradient, including sample loading and column equilibration times. Data was acquired in data-independent mode using Xcalibur 4.5 software. MS1 Spectra were measured with a resolution of 120,000, an AGC target of 2e4, and a mass range from 350 to 1600 m/z. Per MS1, 15 equally distanced, sequential segments were triggered at a resolution of 30,000, an AGC target of 3e6, a segment width of 84 m/z, and a fixed first mass of 200 m/z. The stepped collision energies were set to 22.5, 25, and 27.

All raw data were analyzed with Spectronaut software version 17.2[52] using directDIA analysis methodology and a UniProt database (*Schizosaccharomyces pombe*, UP000002485). Carbamidomethylation on cysteines was set as a fixed modification. Oxidation of methionine and protein N-terminal acetylation were set as variable modifications. Trypsin/P was set as the digestion enzyme.

Please cite this article in press as: Toda et al., Mrc1 regulates parental histone segregation and heterochromatin inheritance, Molecular Cell (2024), https://doi.org/10.1016/j.molcel.2024.07.002

AlphaFold calculations

LocalColabFold[53] was used to predict models of protein complexes. The models were manually examined with PyMOL and Coot.[54]

Protein-protein interaction assay

Residues 781-851 of Mrc1 were cloned into a pGEX vector. The expression plasmid was transformed into Rosetta cells and protein expression was induced using 0.15 mM isopropyl-1-thio-D-galactopyranoside. After incubation at 30°C for 3 hours, the cells were harvested and resuspended in lysis buffer (50 mM sodium phosphate, 300 mM NaCl, pH 7.0), supplemented with 2 mM β-mercaptoethanol and lysed with ultrasonication. The lysate was incubated with Glutathione Sepharose 4B (GE health care) and then washed with lysis buffer. Bound protein was eluted with lysis buffer containing 50 mM glutathione.

Log phase yeast cells expressing Mcm2-FLAG or Mcm2-G221V-FLAG were harvested and washed with 2xHC buffer (300 mM HEPES-KOH at pH 7.6, 2 mM EDTA, 100 mM KCl, 20% glycerol, 0.1% NP40, 2 mM DTT, 1mM PMSF) and frozen in liquid nitrogen. Crude cell extracts were prepared by vigorously blending frozen yeast cells with dry ice using a household blender, followed by incubation with 1xHC buffer containing 250 mM KCl for 30 minutes. The lysate was cleared by centrifugation at 20,000g for 1 hour. The supernatants were incubated with FLAG-agarose beads (Sigma) overnight and washed eight times with 1xHC containing 250 mM KCl.

Protein binding assays were performed by incubating recombinant GST-Mrc1-781-851 with FLAG-agarose beads containing affinity-purified Mcm2-FLAG, Mcm2-G221-FLAG, or a control purification in binding buffer (150 mM HEPES-KOH at pH 7.6, 1 mM EDTA, 250 mM KCl, 10% glycerol, 0.05% NP40, and 1 mM DTT) for 30 minutes at 25°C. The beads were washed six times in binding buffer. The proteins bound to the beads were resolved by SDS-PAGE and detected by western blot analysis.

QUANTIFICATION AND STATISTICAL ANALYSIS

The statistical tests of eSPAN bias were performed using R software. The error bar in the bar plot is the standard error from repeats. The interval of the line plot is the 95% confidence interval of mean value, which is about mean ± 2* standard error. The statistical test of ChIP-qPCR were performed with a unpaired *t* test to calculate two-tailed *p* values.